Semiclassical evaluation of kinetic isotope effects in 13-atomic system

M. Kryvohuz and R. A. Marcus

Citation: J. Chem. Phys. **137**, 134107 (2012); doi: 10.1063/1.4754660
View online: http://dx.doi.org/10.1063/1.4754660
View Table of Contents: http://jcp.aip.org/resource/1/JCPSA6/v137/i13
Published by the American Institute of Physics.

Semiclassical evaluation of kinetic isotope effects in 13-atomic system

M. Kryvohuz[a] and R. A. Marcus[b]
Arthur Amos Noyes Laboratory of Chemical Physics, 127-72, California Institute of Technology, Pasadena, California 91125, USA

(Received 3 August 2012; accepted 10 September 2012; published online 3 October 2012)

The semiclassical instanton approach discussed by Kryvohuz [J. Chem. Phys. **134**, 114103 (2011)] is applied to calculate kinetic H/D isotope effect (KIE) of intramolecular hydrogen transfer in *cis*-1,3-pentadiene. All 33 vibrational degrees of freedom are treated quantum mechanically with semiclassical approximation. Nuclear quantum effects such as tunneling under the barrier and zero-point energy are automatically incorporated in the theory, and are shown to be responsible for the observed appreciable kinetic isotope effect in *cis*-1,3-pentadiene. Over the barrier passage is also automatically included. Numerical calculations are performed on an empirical valence bond potential energy surface and compared with the previous experimental and theoretical studies. An estimation of heavy-atom $^{12}C/^{13}C$ KIE in the same system is also provided and the factors contributing to it are discussed.
 [http://dx.doi.org/10.1063/1.4754660]

I. INTRODUCTION

Proton, hydrogen, and hydride transfer reactions play important roles in many chemically and biologically important processes. Due to the light mass of transferring hydrogen atom, nuclear quantum effects such as tunneling and zero-point energy (ZPE) may play a significant role. Recent experimental and theoretical studies showed the occurrence of tunneling in reactions of enzyme catalysis,[1] which emphasized the importance of nuclear quantum effects in hydrogen transfer reactions.[2–7]

One of the most direct experimental tools for the assessment of the mechanism of hydrogen transfer is measurement of kinetic isotope effects (KIE).[8] The KIE is the ratio of rates of two reactant isotopologues, which in case of hydrogen transfer is usually the ratio of the rate of hydrogen transfer to the rate of deuterium transfer, k_H/k_D, or to the rate of tritium transfer, k_H/k_T. Large values of KIE can be indicators of significant quantum effects.[7,9,10] Nuclear zero-point energy effects can result in the values of KIE up to $k_H/k_D = 7$ at room temperatures,[11,12] while higher values of KIE suggest involvement of quantum mechanical tunneling in the mechanism of hydrogen transfer.[13–16] A KIE close to 100 has been experimentally observed in reactions of enzyme catalysis even at physiological temperatures,[17] and KIE of more than 400 has been reported for a non-enzymatic system.[18] Development of an adequate theoretical approach for quantitative description of KIEs is of much interest for understanding the physical origin of the observed KIEs and mechanisms of the underlying chemical reactions.

For quantitative description of KIEs it is necessary to employ a reaction rate theory that incorporates quantum mechanical effects. Several quantum reaction rate theories exist and have been tested on multiple chemical and biological systems.[19–27] For a given potential energy surface (PES), the quantum instanton approach[22] provides accurate estimates of quantum mechanical reaction rates.[28,29] However, it requires considerable statistical sampling on the order 10^7 points[30,31] and thus may need a priori knowledge of PES. On the other hand, in cases when PES is not known, or when a direct path integral approach requires a considerable computational effort, a simplified way of rate constant estimation looks attractive.[20,32] One of such methods is based on the semiclassical instanton theory,[21,33–46] and is capable of accounting for nuclear quantum effects such as zero-point energy and tunneling. Another merit of the instanton approach is that it provides more conceptual insight on the role of nuclear quantum effects, and tunneling in particular, in the mechanism of a chemical reaction. It does not involve *ad hoc* approximations of tunneling phenomena and thus can provide an automated method for rigorous evaluation of chemical reaction rate constants and KIEs in multiatomic systems. A quantitative advantage of the semiclassical instanton approach is its dependence on a single $\hbar\beta$-periodic classical trajectory. These trajectories are sufficiently easy to find using methodology described in the present paper or other methods.[40,45,48] While for known PES, the semiclassical instanton approach can provide a simple and rather accurate estimate of quantum reaction rate constants, for molecular systems with unknown PES the determination of instanton trajectories can be efficiently combined with on the fly *ab initio* calculations of PES, which has been already successfully implemented in Refs. 47, 49, and 50.

A major limitation of semiclassical instanton theory was the restriction of its applicability only to low-temperature systems. We have recently proposed an extension of the semiclassical instanton method[51] which can be applied at any temperature and checked its validity for the estimation of quantum reaction rate constants of several atom-diatom scattering reactions. Although the semiclassical instanton approach underestimated reaction rate constants by a factor of 1.5−2, which is primarily due to the neglect of anharmonicity effects of the orthogonal to the reaction coordinate degrees of freedom,[51,52] this factor remains the same for different isotopologues of

[a]Electronic mail: mkryvohuz@anl.gov.
[b]Electronic mail: ram@caltech.edu.

reacting species. We thus expect that the semiclassical instanton approach can provide accurate estimates of KIEs. In this paper we test the performance of the semiclassical instanton method for calculation of kinetic isotope effects of intramolecular hydrogen transfer in *cis*-1,3-pentadiene.[53–56] The KIEs of 4 to 5 have been experimentally observed in this system in the temperature range of 460−500 K,[57] and the importance of quantum tunneling has been emphasized for this reaction.[53,54] We calculate KIE by comparing the rate constants of H transfer in the same isotopologues that were measured in experiment: hydrogen transfer in $D_2C(CH)_3CH_3$ and deuterium transfer in $H_2C(CH)_3CD_3$. We also study heavy atom $^{12}C/^{13}C$ KIEs of H transfer in $D_2C(CH)_3CH_3$. Due to the importance of skeleton motions and possible dynamical effects of environment on hydrogen transfer step in reactions of enzyme catalysis,[58] this multidimensional 13-atomic system may serve as a prototype of hydrogen transfer in enzyme reactions, particularly in approaches where a subset of the atoms ∼50 is treated quantum mechanically and the rest by other methods.[1,10,59,60]

The paper is organized as follows. In Sec. II the semiclassical instanton approach is reviewed and the key equations (2.1) and (2.2) of the paper are provided. In Sec. III, the type of potential energy surface used in calculations is discussed. In Secs. IV and V the algorithm for the search of instanton trajectories is discussed and the results of numerical calculations of H/D and heavy-atom KIEs are presented. The paper is concluded in Sec. VI with a discussion of the results and suggestions for the future improvements and applications of the present approach.

II. SEMICLASSICAL INSTANTON APPROACH

The semiclassical instanton approach can be considered as a multidimensional generalization of the semiclassical WKB theory.[61] This approach is based on determination of particular classical periodic trajectories, called instantons, on inverted potential energy surfaces. Instantons correspond to oscillations along a single stable degree of freedom which originates from the unstable degree of freedom (the reaction coordinate) after inversion of PES.[33] These periodic trajectories make dominant contributions to the quantum partition function path integrals allowing one to evaluate them within a stationary phase approximation. Classical parameters corresponding to instanton trajectories, such as energy E_{inst}, action $\mathcal{W}_{inst}$, and stability parameters λ_n enter the resulting semiclassical expressions and provide an estimate for the quantum parameter of interest such as reaction rate constant or ground state energy splitting.[33,35,40,41,62–69]

In Ref. 51, the following semiclassical expressions for reaction rate constants k were proposed based on the instanton theory

$$k = \frac{\kappa_B T}{h}\frac{Q_{vib}}{Q_r}e^{-\frac{\mathcal{W}_{inst}(\beta)}{\hbar}} \times \left\{\sqrt{2\pi\frac{\mathrm{d}\widetilde{E}(\beta)}{\mathrm{d}(1/\beta)}}\,\mathrm{erf}\left[\frac{\widetilde{V}_0-\widetilde{E}(\beta)}{\sqrt{-\mathrm{d}\widetilde{E}(\beta)/\mathrm{d}\beta}}\right]\right\}, \quad \text{for } \beta \geq \widetilde{\beta}_c \tag{2.1}$$

$$k = \frac{1}{Q_r}\frac{\mathrm{Corr}(\Delta)}{2\hbar\widetilde{\beta}_c\sin(\pi\beta/\widetilde{\beta}_c)}e^{-\beta\widetilde{V}_0}, \quad \text{for } \beta \leq \widetilde{\beta}_c, \tag{2.2}$$

where $\widetilde{\beta}_c$ is the crossover parameter defined in Eq. (2.8) which separates high-temperature and low-temperature regimes; Q_r is the partition function of the reactants and

$$Q_{vib} = \exp(-\beta F_{vib}) \tag{2.3}$$

is the partition function of orthogonal to the reaction coordinate oscillators (transverse degrees of freedom).

$$F_{vib}(\beta) = \frac{1}{\beta}\sum_{n=1}^{N-1}\ln\left(2\sinh\frac{\lambda_n(\beta)}{2}\right) \tag{2.4}$$

is the effective total free energy of transverse degrees of freedom.

$$\widetilde{E}(\beta) = E_{inst}(\beta) + E_{vib} \tag{2.5}$$

is the total vibrational energy, in which E_{inst} is the vibrational energy associated with the instanton trajectory and E_{vib} is the vibrational energy of transverse degrees of freedom given by the Gibbs-Helmholtz expression

$$E_{vib} = \frac{\mathrm{d}}{\mathrm{d}\beta}(\beta F_{vib}(\beta)). \tag{2.6}$$

The factor $\mathrm{Corr}(\Delta)$ accounts for the anharmonicity of the effective one-dimensional potential barrier along the reaction coordinate at high temperatures[41] and is given by

$$\mathrm{Corr}(\Delta) = \Delta\sqrt{2\pi}\,\mathrm{erf}(-\Delta)e^{\Delta^2/2}$$
$$\Delta = \frac{\beta}{2}\left(\left(\frac{\widetilde{\beta}_c}{\beta}\right)^2 - 1\right)\sqrt{-\mathrm{d}\widetilde{E}(\widetilde{\beta}_c)/\mathrm{d}\beta}. \tag{2.7}$$

The expression in curly brackets in Eq. (2.1) stands for the anharmonicity of the barrier along the reaction coordinate at tunneling temperatures $\beta > \widetilde{\beta}_c$.[70] It also contains the error function $\mathrm{erf}(\Delta) \equiv (1/\sqrt{2\pi})\int_{-\infty}^{\Delta}\exp(-x^2/2)dx$ which truncates spectrum of energies available for tunneling at the barrier top.

The above parameters $E_{inst}(\beta) = -\frac{1}{2}\dot{\mathbf{x}}^2 + V(\mathbf{x})$, $\mathcal{W}_{inst}(\beta) = \int_0^{\hbar\beta}[\frac{1}{2}\dot{\mathbf{x}}(\tau)^2 + V(\mathbf{x}(\tau))]d\tau$, and $\lambda_n(\beta)$ are calculated along the $\hbar\beta$-periodic classical trajectory, the instanton, on inverted N-dimensional reactive PES in mass-scaled coordinates and are functions of the inverse temperature $\beta \equiv 1/\kappa_B T$. $\widetilde{V}_0 \equiv \widetilde{E}(\widetilde{\beta}_c)$ is the effective barrier height, which includes zero-point energy contributions of the $N-1$ degrees of freedom orthogonal to the reaction coordinate. The crossover inverse temperature $\widetilde{\beta}_c$ is the root of equation

$$\widetilde{\mathcal{W}}(\beta) - \hbar\beta\widetilde{E}(\beta) = 0, \tag{2.8}$$

where we have defined an effective total Euclidian action

$$\widetilde{\mathcal{W}}(\beta) = \mathcal{W}_{inst}(\beta) + \hbar\beta F_{vib}(\beta). \tag{2.9}$$

Equation (2.8) is equivalent to zero value of the effective WKB action (or the abbreviated action) $\widetilde{W} \equiv 2\int_a^b \dot{s}ds = 0$ along the reaction coordinate s. The latter occurs when the

two real semiclassical turning points a and b coincide at the barrier top, $a = b$. Physically $\widetilde{\beta}_c$ corresponds to the temperature above which an optimal tunneling path disappears, and tunneling effects become non-dominant (although the effects of over-the-barrier reflections and non-dominant tunneling contributions are rigorously present in Eqs. (2.1) and (2.2) as discussed further in this section).

The meaning of the parameters in Eqs. (2.1)–(2.7) is the following. Equations (2.1) and (2.2) describe the rate of reactive flux over some one-dimensional potential barrier, to which an arbitrary multidimensional system with a first-order saddle point can be reduced. This one-dimensional barrier consists of a barrier along the effective reaction coordinate, the instanton, which is determined in numerical calculations, plus zero-point vibrational energies $\frac{d}{d\beta}(\beta F_{vib}(\beta))$ of degrees of freedom orthogonal to the reaction coordinate. Stability parameters λ_j, $j = 1, \ldots, N-1$ along the instanton trajectory effectively stand for the vibrational frequencies $\lambda_j/\hbar\beta$ of $N-1$ transverse degrees of freedom. The properties that correspond to the effective one-dimensional barrier are denoted with tilde-hats, i.e., $\widetilde{E}$, $\widetilde{\mathcal{W}}$, etc., while the properties that correspond to the instanton trajectories on the original PES (i.e., before adding the contribution of orthogonal degrees of freedom) are denoted with the *inst* subscript, such as E_{inst}, $\mathcal{W}_{inst}$, etc. The quantities $\widetilde{\mathcal{W}}$ and $\widetilde{E}$ stand for the combined Euclidian action and the corresponding energy under an effective one-dimensional potential barrier. The height $\widetilde{V}_0$ of this effective barrier is given by the maximum value that $\widetilde{E}$ can take. The parameter $\widetilde{\beta}_c$ defines the unstable harmonic frequency at the top of the effective potential barrier $\widetilde{\omega}_b = 2\pi/\hbar\widetilde{\beta}_c$. Equations (2.1)–(2.5) are governed by $E_{inst}(\beta)$, $\mathcal{W}_{inst}(\beta)$, and $\lambda_n(\beta)$. Once such trajectories are determined for given β's, Eqs. (2.1) and (2.2) provide an estimate of quantum reaction rate constant k. At $\widetilde{T}_c = 1/\kappa\widetilde{\beta}_c$, i.e., at $\beta = \beta_c$, both expressions give the same value of k.[41,51]

Instanton trajectories can be assigned a physical meaning, they represent the optimal tunneling path at a given temperature under a multidimensional barrier, i.e., under a given multidimensional PES with a first-order saddle point. For a general anharmonic barrier, longer oscillation periods of classical periodic trajectories in the inverted barrier correspond to spatially longer trajectories, as seen in Fig. 1. Hence, lower temperatures (higher values of β) correspond to longer $\hbar\beta$-periodic trajectories, and thus longer tunneling paths. When β decreases, so does the corresponding period $\hbar\beta$ of the instanton. The minimum period of classical periodic motion in a general anharmonic well usually corresponds to oscillations around its minimum (or in case of an inverted barrier to the maximum of the barrier), as it can be seen in Fig. 1. Therefore at some crossover temperature, T_c, instantons shrink down to the saddle point, which means that at this and higher temperatures instantons, or tunneling paths, disappear and reaction rate starts to be dominated by over-the-barrier mechanism. We note, however, that, regardless of seemingly simple physical picture of instantons, all important quantum effects of near-the-barrier region such as over-the-barrier reflections are correctly captured by the semiclassical expressions in Eqs. (2.1) and (2.2), for instance, as discussed in Ref. 41. Clearly, the crossover temperature is determined by the shape

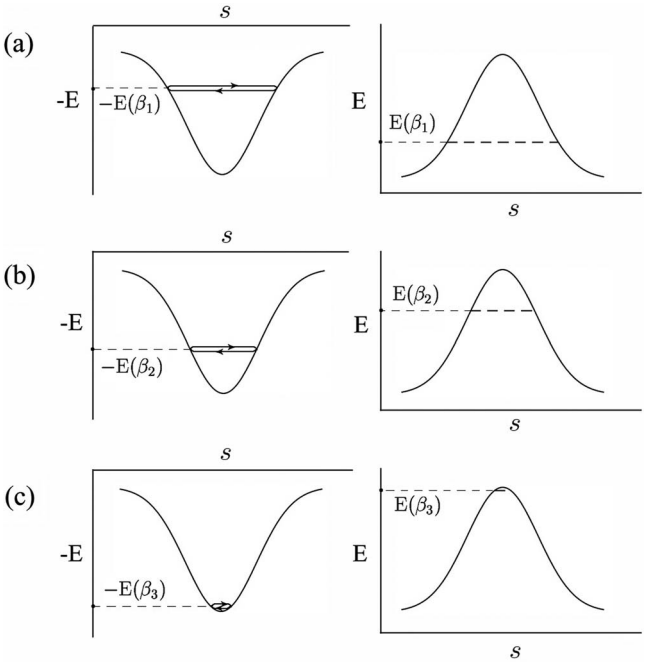

FIG. 1. Schematic representation of the semiclassical instanton approach. A one-dimensional case is shown (which is equivalent to the WKB approach). Potential barrier $V(s)$ along the reaction coordinate s is illustrated in the right column. The left column corresponds to the inverted barrier $-V(s)$, on which $\hbar\beta$-periodic trajectories (instantons) are sought. Rows (a), (b), and (c) illustrate instanton trajectories (left figure) and their corresponding tunneling paths (right figure) at inverse temperatures β_1, β_2, and β_3, respectively, such that $\beta_1 > \beta_2 > \beta_3$. The inverse temperature β_3 lies in the vicinity of the crossover temperature.

of the barrier and is equal to $\hbar\omega_b/2\pi\kappa_B$, where ω_b is the imaginary frequency of the unstable mode at the saddle point. One can say that T_c separates under-the-barrier and over-the-barrier regimes of quantum mechanical reaction rate, yet this transition is obviously smooth, and is quantitatively given by the continuous transition of Eq. (2.1) into Eq. (2.2) in the vicinity of the crossover temperature. (in Ref. 51 we proposed to use $\widetilde{T}_c$ entering Eqs. (2.1) and (2.2) as a crossover temperature instead of T_c, since $\widetilde{T}_c$ appropriately accounts for the additional contribution of the orthogonal to the reaction path degrees of freedom.)

It is interesting to note here beforehand that the range of temperatures, 460–500 K, at which KIEs of H-transfer in *cis*-1,3-pentadiene were measured,[57] is already above its corresponding crossover temperature, which means that the tunneling mechanism is not the primary mechanism of the H-transfer reaction. Yet, it still considerably contributes to the overall KIE increasing it by a factor of 2 as we show further in this paper.

III. POTENTIAL ENERGY SURFACE

It follows from the discussion in Sec. II that the shape of PES, and more importantly its region near the saddle point, determines how much tunneling contributes to the quantum mechanical reaction rate constant. In particular, the crossover temperature T_c, that separates under-the-barrier and over-the-barrier regimes of the quantum reaction rate, depends on the

frequency of the unstable mode at the transition state. For a quantitative description of KIEs one therefore needs some accurate, preferably *ab initio*, PES. Previous theoretical studies of hydrogen transfer in *cis*-1,3-pentadiene molecule[55] successfully reproduced experimental KIEs using empirical valence bond (EVB) PES.[71,72] In the present paper we use the same PES to test the performance of the present semiclassical instanton approach.

Following the Ref. 55, EVB potential is constructed by taking the lower eigenvalue of the 2×2 matrix $\left(\begin{smallmatrix} V_{11} & V_{12} \\ V_{21} & V_{22} \end{smallmatrix}\right)$:

$$V_{\mathrm{EVB}} = \frac{1}{2}(V_{11} + V_{22}) - \sqrt{|V_{12}|^2 + \left(\frac{V_{11} - V_{22}}{2}\right)^2}, \quad (3.1)$$

in which V_{11} is a potential surface of the diabatic reactants state and V_{22} is a potential surface of the diabatic products state. The coupling term V_{12} is taken to be such that the EVB potential $V_{\mathrm{EVB}}(\mathbf{r})$ matches the accurate electronic PES in the vicinity of the transition state configuration, i.e., the barrier height, the gradient, and the Hessian of $V_{\mathrm{EVB}}(\mathbf{r})$ in the transition state configuration should match those obtained from *ab initio* electronic structure calculations. For this reason, the EVB approach is convenient for our purposes since at non-cryogenic temperatures instanton trajectories are concentrated in the vicinity of the saddle point, as in Fig. 1(c). Thus, we need an accurate description of PES only in the vicinity of the saddle point. Yet, one needs to keep in mind that instanton trajectories of different periods $\hbar\beta$ can exist only if PES is anharmonic. If the saddle point region was completely harmonic with some constant unstable frequency ω_0, then only instantons of period $\hbar\beta = 2\pi/\omega_0$ could exist on the corresponding inverted PES. The latter means that, technically speaking, the information of only accurate gradient and Hessian at the saddle point is not sufficient to appropriately describe the saddle point region, since it is anharmonicity that makes instanton trajectories different. The presence of anharmonicity along the reaction coordinate has been assumed in the derivation of Eq. (2.1). The dependence of reaction rate constants on this anharmonicity is not surprising, since quantum rate constants in harmonic approximation diverge at temperatures below the crossover temperature. For this reason a simple harmonic quantum transition state is inadequate for describing the quantum activated rate process by this method.[41] Yet, since the present PES has successfully reproduced KIEs in Ref. 55, we assume that anharmonicity effects in the vicinity of the saddle point are correctly captured by the EVB potential of Eq. (3.1).

Potentials $V_{11}(\mathbf{r})$ and $V_{22}(\mathbf{r})$ are taken as molecular mechanics potentials of the GAFF force field of the AMBER molecular dynamics package:[73,74]

$$\begin{aligned} V(\mathbf{r}) = &\sum_{\text{bonds}} K_r(r - r_{eq})^2 + \sum_{\text{angles}} K_\theta(\theta - \theta_{eq})^2 \\ &+ \sum_{\text{dihedrals}} \frac{V_n}{2}[1 + \cos(n\phi - \gamma)] \\ &+ \sum_{\text{nonbonded pairs } i<j} \left(\frac{A_{ij}}{r_{ij}^{12}} - \frac{B_{ij}}{r_{ij}^{6}} + \frac{q_i q_j}{r_{ij}}\right), \end{aligned} \quad (3.2)$$

where the first term stands for bond stretches, the second term for angle bends, the third term for dihedral angles, and the last term represents van der Waals and Coulomb interactions between nonbonded pairs of atoms. The same modifications as in Ref. 55 were introduced to the force field in Eq. (3.2): first, the harmonic bond stretch potential of the bond been broken was replaced with the Morse potential with the dissociation energy of C-H bond; and second, the nonbonded interaction of the bond been formed was omitted in order to reduce its divergent contributions to the EVB potential (3.1).

The coupling term $V_{12}(\mathbf{r})$ is taken in the form[55]

$$V_{12}^2(\mathbf{r}) = A \exp[1 + \mathbf{B}\cdot\Delta\mathbf{r} + (1/2)\Delta\mathbf{r}\cdot(\mathbf{C} + \alpha\mathbf{I})\cdot\Delta\mathbf{r}], \quad (3.3)$$

where $\Delta\mathbf{r} = \mathbf{r} - \mathbf{r}_{\mathrm{TS}}$ is a displacement from the transition state configuration $\mathbf{r}_{\mathrm{TS}}$, i.e., the saddle point, and scalar A, vector $\mathbf{B}$ and matrix $\mathbf{C}$ are determined as follows:[75]

$$\begin{aligned} A &= [V_{11}(\mathbf{r}_{\mathrm{TS}}) - V(\mathbf{r}_{\mathrm{TS}})][V_{22}(\mathbf{r}_{\mathrm{TS}}) - V(\mathbf{r}_{\mathrm{TS}})], \\ \mathbf{B} &= \frac{\mathbf{D}_1}{[V_{11}(\mathbf{r}_{\mathrm{TS}}) - V(\mathbf{r}_{\mathrm{TS}})]} + \frac{\mathbf{D}_2}{[V_{22}(\mathbf{r}_{\mathrm{TS}}) - V(\mathbf{r}_{\mathrm{TS}})]}, \\ \mathbf{D}_n &= \left.\frac{\partial V_{nn}(\mathbf{r})}{\partial \mathbf{r}}\right|_{\mathbf{r}=\mathbf{r}_{\mathrm{TS}}} - \left.\frac{\partial V(\mathbf{r})}{\partial \mathbf{r}}\right|_{\mathbf{r}=\mathbf{r}_{\mathrm{TS}}} \\ \mathbf{C} &= \frac{\mathbf{D}_1\mathbf{D}_2^{\mathrm{T}} + \mathbf{D}_2\mathbf{D}_1^{\mathrm{T}}}{A} + \frac{\mathbf{K}_1}{V_{11}(\mathbf{r}_{\mathrm{TS}}) - V(\mathbf{r}_{\mathrm{TS}})} \\ &\quad + \frac{\mathbf{K}_2}{V_{22}(\mathbf{r}_{\mathrm{TS}}) - V(\mathbf{r}_{\mathrm{TS}})}, \\ \mathbf{K}_n &= \left.\frac{\partial^2 V_{nn}(\mathbf{r})}{\partial \mathbf{r}^2}\right|_{\mathbf{r}=\mathbf{r}_{\mathrm{TS}}} - \left.\frac{\partial^2 V(\mathbf{r})}{\partial \mathbf{r}^2}\right|_{\mathbf{r}=\mathbf{r}_{\mathrm{TS}}}. \end{aligned} \quad (3.4)$$

The parameter α in Eq. (3.3) was taken to be 0.9 a.u. as suggested in Ref. 55. To summarize, the EVB PES used is built to match the exact quadratic form at the saddle point. The rest of the surface is approximated via the classical molecular mechanics force field, which is overall anharmonic. The resulting PES is therefore anharmonic (inseparable) everywhere except for the saddle point.

The optimized transition state configuration, $\mathbf{r}_{\mathrm{TS}}$, the barrier height $V(\mathbf{r}_{\mathrm{TS}})$, the gradient $\frac{\partial V(\mathbf{r})}{\partial \mathbf{r}}|_{\mathbf{r}=\mathbf{r}_{\mathrm{TS}}}$, and the Hessian $\frac{\partial^2 V(\mathbf{r})}{\partial \mathbf{r}^2}|_{\mathbf{r}=\mathbf{r}_{\mathrm{TS}}}$ in the transition state configuration were obtained from electronic structure calculations. The latter were performed with JAGUAR software package[76] using MPW1K/6-31+G(d,p) method. The search for the minimum energy configurations was then performed and resulted in the barrier height of 36.05 kcal/mol between the s-*cis* isomer of pentadiene and the transition state configuration. The unreactive s-*trans* conformer is 3.29 kcal/mol lower in energy than the s-*cis* one. The s-*trans* confomer is therefore the reactant in the overall sigmatropic rearrangement reaction, which in the course of reaction transforms into the s-*cis* conformer by internal rotation followed by the H-transfer step.[54] The calculated frequencies of $D_2C(CH)_3CH_3$ and $H_2C(CH)_3CD_3$ isotopologues, used in experiment,[57] in their minimum energy

TABLE I. Calculated vibrational frequencies of isotopologues of C_5H_8 in cm^{-1}.

$D_2C(CH)_3CH_3$			$H_2C(CH)_3CD_3$		
Min. energy (*trans*)	Min. energy (*cis*)	Transition state	Min. energy (*trans*)	Min. energy (*cis*)	Transition state
3266.13	3337.69	3282.36	3334.48	3253.7	3282.35
3255.03	3253.87	3271.79	3264.03	3235.01	3271.71
3236.00	3246.43	3245.83	3254.36	3225.58	3245.79
3222.96	3233.18	3241.6	3237.23	3179.15	3241.59
3174.31	3224.66	3195.99	3232.01	3130.21	3195.98
3113.94	3197.08	2432.09	2390.83	2485.91	2432.05
2483.52	2351.38	2327.58	2349.29	2374.39	2327.49
2370.08	2271.19	1644.32	2241.93	2341.81	1632.44
1790.23	1774.71	1621.87	1793.07	1774.75	1606.4
1683.58	1758.28	1565.07	1725.09	1710.44	1552.21
1525.72	1504.78	*i* 1563.27	1511.76	1500.76	1477.25
1517.27	1468.23	1528.54	1435.04	1477.19	1303.18
1476.0	1363.15	1485.18	1357.62	1368.79	1295.6
1442.38	1352.36	1406.61	1317.14	1358.23	*i* 1237.89
1340.04	1333.36	1305.3	1222.22	1328.54	1205.49
1318.19	1301.94	1295.76	1150.98	1288.63	1181.86
1213.14	1148.59	1201.02	1096.33	1114.92	1162.96
1098.98	1120.93	1161.22	1094.57	1066.84	1120.69
1088.20	1076.26	1109.8	1069.75	1042.73	1071.21
1051.63	1060.39	1061.27	1033.79	1033.47	1038.19
1046.69	1051.	1033.79	995.50	1017.38	1017.33
994.93	987.116	1028.74	974.54	997.33	991.859
970.32	948.72	982.515	930.38	921.414	965.296
810.59	913.277	900.123	921.03	846.482	891.066
792.22	847.42	890.359	837.22	794.93	881.233
764.24	776.26	810.63	798.60	755.122	782.781
619.12	701.657	781.021	629.05	635.693	770.734
574.66	582.608	697.201	576.15	546.384	690.851
364.98	427.329	568.976	381.52	390.676	565.666
342.79	328.756	555.328	352.16	312.706	549.027
213.13	228.146	498.198	209.61	220.585	496.877
129.65	166.902	450.117	129.63	164.103	437.228
109.30	102.432	260.544	85.11	106.331	260.139

and the transition state configurations are listed in Table I. These frequencies are then used to calculate reactants partition function $Q_r = \prod_{j=1}^{33} 1/2\sinh(\hbar\omega_j\beta/2)$ that enters Eqs. (2.1) and (2.2).

IV. INSTANTON TRAJECTORIES IN INTERNAL COORDINATES

Pentadiene molecule has 39 degrees of freedom, 3 of which are translational, 3 rotational, and 33 vibrational. These 33 vibrational degrees of freedom constitute a 33-dimensional space of internal coordinates in which instanton trajectories are sought. Overall translations do not make any influence on the internal vibrational dynamics, while overall rotations may interact with vibrations through the centrifugal and Coriolis coupling. Therefore, identification of instanton trajectories in molecules with unrestricted rotations requires appropriate account of vibrational-rotational interactions. Rigorous treatment of rovibrational coupling in semiclassical instanton theory has been developed by Mil'nikov and Nakamura in Refs. 42 and 69. They have successfully applied semiclassical instanton approach to calculate coherent tunnel splittings of degenerate ground state energy levels in multiatomic molecules. Interactions of instanton trajectories with rotations were treated by searching for instantons in curvilinear system of internal coordinates, which is a nontrivial task. Fortunately, our situation is somewhat different. The instanton trajectories that arise in the theory of coherent tunnel splitting have infinite period of classical motion and correspond to the infinite value of inverse temperature β. Yet, the instanton trajectories that are needed for the theory of chemical reaction rates correspond to finite (physiological) values of β. The latter implies that instanton trajectories of the semiclassical reaction rate theory discussed in the present paper are spatially much shorter (as seen in the comparison of Figures 1(c) and 1(a)), and thus the corresponding vibrational motion along the instanton trajectories has significantly smaller amplitude (tight transition state is assumed in the present paper). For vibrations of small amplitude we can separate vibrational motion from rotations and search for instanton trajectories in non-rotating molecule while treating molecular rotations as those of a rigid body, as shown below.

The Watson molecular Hamiltonian[77] of a semi-rigid molecule has a compact form in the normal mode coordinates $\{P_k, Q_k\}$ and reads

$$H = \frac{1}{2}\sum_{k=1}^{3N-6} P_k^2 + V(Q_1, \ldots, Q_{3N-6}) + \frac{1}{2}\sum_{\alpha,\beta=1}^{3} \mu_{\alpha\beta}(J_\alpha - \pi_\alpha)(J_\beta - \pi_\beta) - \frac{\hbar^2}{8}\sum_{\alpha=1}^{3}\mu_{\alpha\alpha}, \tag{4.1}$$

where J_α and π_α are components of the rotational and vibrational angular momenta, respectively, and $\mu_{\alpha\beta}$ is the generalized inverse inertia tensor. The first two terms in the Hamiltonian (4.1) correspond to internal vibrations, the third term correspond to the Coriolis coupling of vibrations and rotations, and the last term is a small correction that appears in the expression of Watson Hamiltonian. It is known that the standard rectilinear normal coordinates automatically enforce Eckart conditions,[78] which minimize vibrational angular momentum and make it zero at equilibrium. For small-amplitude motion around equilibrium configuration, we can therefore omit vibrational angular momentum in the molecular Hamiltonian and obtain

$$H = \frac{1}{2}\sum_{k=1}^{3N-6} P_k^2 + V(Q_1, \ldots, Q_{3N-6}) + \frac{1}{2}\sum_{\alpha,\beta=1}^{3} \mu_{\alpha\beta} J_\alpha J_\beta - \frac{\hbar^2}{8}\sum_{\alpha=1}^{3}\mu_{\alpha\alpha}. \tag{4.2}$$

For a moderate size molecule, small amplitude vibrational motion does not make a significant perturbation on the magnitude of $\mu_{\alpha\beta}$. The latter separates rotations from vibrations as can be seen from Eq. (4.2). At this point, no assumptions were made on the form of the potential $V(Q_1, \ldots, Q_{3N-6})$ itself which still contains anharmonic couplings of vibrational normal modes. One can argue that Coriolis coupling of vibrational modes may be comparable to the potential anharmonic coupling, however, experimental studies of intramolecular vibrational energy relaxation in small organic molecules[79,80] suggests that Coriolis coupling is much weaker than the anharmonic mode coupling. The latter is partly due to the large moments of inertia of moderate size molecules which make the Coriolis term small. We thus conclude that for the present purposes it is sufficient to search for instanton trajectories in a $(3N-6)$-dimensional normal mode space with the vibrational Hamiltonian given by

$$H' = \frac{1}{2}\sum_{k=1}^{3N-6} P_k^2 + V(Q_1, \ldots, Q_{3N-6}). \tag{4.3}$$

We expect that such normal mode representation will remain valid for a general class of instanton trajectories with finite periods that correspond to the temperatures of chemical interest.

To make a canonical transformation from Cartesian coordinates $\{r_{3N}\}$ to normal mode coordinates $\{Q_{3N}\}$ one needs to diagonalize mass weighted Hessian matrix $\mathbf{F} = (1/\sqrt{m_i m_j})\partial^2 V/\partial r_i \partial r_j$ at the equilibrium configuration obtained from the electronic structure calculations of Sec. III. Eigenvectors of the mass weighted Hessian matrix constitute the columns of the tranformation matrix $\mathbf{S}$, such that

$$\Lambda = \mathbf{S}^{\mathrm{T}}\mathbf{F}\mathbf{S}, \tag{4.4}$$

where Λ is a diagonal matrix with the corresponding squared vibrational frequencies along the diagonal. The transformation

$$\vec{Q} = \mathbf{S}^{\mathrm{T}}\vec{x} \tag{4.5}$$

generates a set of internal coordinates $vecQ$ in the body-fixed (Eckart) frame. Vector $\vec{x}_i = \sqrt{m_i}\vec{r}_i$ stands for the mass-weighted Cartesian coordinates. The first 33 coordinates Q that correspond to non-zero eigenvalues of the Hessian constitute vibrational normal modes, while the remaining six coordinates correspond to rotations and translations. Setting these six coordinates to be 0 one can use backward transformation

$$\begin{pmatrix} x_1 \\ y_1 \\ z_1 \\ \ldots \\ x_{13} \\ y_{13} \\ z_{13} \end{pmatrix} = \mathbf{S} \begin{pmatrix} Q_1 \\ Q_2 \\ \ldots \\ Q_{33} \\ 0 \\ \ldots \\ 0 \end{pmatrix} \tag{4.6}$$

to relate instanton trajectories found in the $\{Q_{3N-6}\}$ coordinates with the mass-weighted Cartesian displacements x_{3N} of individual atoms from their equilibrium positions. Zero amplitudes of the latter six zero-frequency normal modes constitute the Eckart conditions imposed on a semirigid molecule for separation of rotations from vibrations.[78] The same Eckart conditions were used in the theoretical study of KIEs in *cis*-pentadiene in Ref. 55.

Since instanton trajectories for the temperatures of interest are concentrated around the saddle point, it is convenient to consider the transition state configuration of the molecule as an equilibrium configuration around which normal mode analysis is performed. One should note again, that the normal mode analysis here is used only to find a set of convenient internal coordinates, which yet are coupled by the anharmonicities of PES.

To search for instanton trajectories, we use a procedure described in Ref. 51, although alternative algorithms are also available.[40,45,48] An $\hbar\beta$-periodic trajectory can be represented in terms of Fourier series with coordinates $\{Q_{3N-6}\}$ in the form

$$Q_n(\tau) = \sum_{j=0}^{\infty} C_j^n \cos\left(\frac{2\pi}{\hbar\beta} j\tau\right). \tag{4.7}$$

The real unknown coefficients C_j^n are to be found from the solution of $\delta S(\vec{C}) = 0$ by running Newton-Raphson optimization algorithm for the Euclidian action

$$S(\vec{C}) = \sum_{n=1}^{33}\int_0^{\hbar\beta}\left(\frac{\dot{Q}_n^2}{2} + V(\vec{Q}(\vec{C}))\right)d\tau. \tag{4.8}$$

Starting with $\vec{Q} = \vec{C}_0$ one can add higher-order coefficients $C_1^n, C_2^n, \ldots$ one by one to obtain the instanton trajectory $Q_n(\tau)$

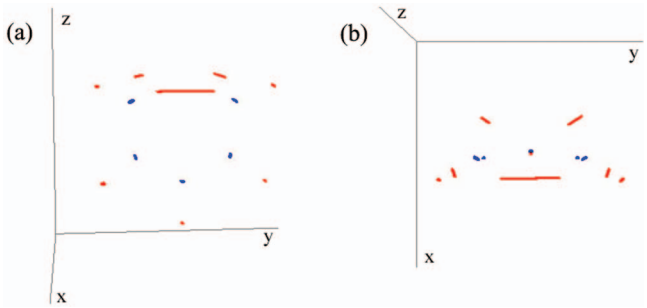

FIG. 2. Instanton trajectory in $D_2C(CH)_3CH_3$ at 352 K determined on the EVB PES of Sec. III. The trajectory is scaled five times to be visible, i.e., Fourier coefficients C_j in Eq. (4.7), $j > 1$ are multiplied by the factor of 5. The red lines stand for tunnel paths of H(D) atoms, the blue lines stand for tunnel paths of C atoms. (a) front view, (b) top view.

of arbitrary precision for any given inverse temperature β.[51] In practice, it is convenient to start with assigning 2 to 3 lowest order Fourier coefficients to the unstable normal mode while keeping the rest of normal modes fixed and run one round of optimization. Then to unfix some of the remaining stable modes by assigning them the lowest order coefficient C_0^n. After converging optimization algorithm with this number of coefficients, higher order Fourier coefficients can be added in the following rounds of optimization.

The Fourier coefficients C_j^n have an interesting physical meaning. Zero-order Fourier coefficients C_0^n indicate collective reorganization of atoms to promote tunneling. While higher order coefficients C_j^n, $j > 0$ indicate the degree to which a particular normal mode participates in tunneling. A typical instanton trajectory is shown in Figure 2 and represents the collective tunneling of atoms in $D_2C(CH)_3CH_3$ at 352 K.

V. KINETIC ISOTOPE EFFECTS

Kinetic isotope effect is determined as the ratio k_H/k_D of the reaction rate constant for the reaction of hydrogen transfer to that of deuterium transfer. We calculate the rate constants of hydrogen and deuterium transfer for the same isotopologues, $D_2C(CH)_3CH_3$ and $H_2C(CH)_3CD_3$ of *cis*-1,3-pentadiene, respectively, that were measured experimentally.[57]

From Table I it follows that the crossover temperature $T_c = \hbar\omega_b/2\pi\kappa_B$, (here ω_b is the unstable frequency at the transition state), at which instanton trajectories collapse to the saddle point is 358 K for $D_2C(CH)_3CH_3$ and 283 K for $H_2C(CH)_3CD_3$. The experimentally reported range of temperatures 460−500 K is above both of these crossover temperatures, which means that within this range of temperatures the reactions of hydrogen and deuterium transfer are dominated by over-the-barrier mechanisms. Yet, tunneling can still make a significant contribution since the crossover temperature, 358 K, of $D_2C(CH)_3CH_3$ is not too far from the reported temperature range.

The fact that the temperature range of interest is above the instanton crossover temperature implies that Eq. (2.2) should be used for evaluation of semiclassical reaction rate constants. It is interesting that Eq. (2.2) depends only on three constant parameters $\widetilde{\beta}_c$, $\widetilde{V}_0$, and $E'(\widetilde{\beta}_c)$. Once these parameters are determined from instanton analysis, Eq. (2.2) provides an analytical expression for the reaction rate constant at any temperature above the crossover one.

Equation (2.2) needs to be modified to include overall rotations, since its original version was derived only on the basis of internal coordinates. Using the correspondence between the semiclassical instanton approach and the transition state theory,[33,51] contribution of rotations can be accounted for by multiplying Eq. (2.2) by the ratio of rotational partition functions $Q^{\ddagger}_{rot}/Q^{r}_{rot}$ at the transition state and reactants state, respectively. The resulting semiclassical expression for the rate constant of the hydrogen transfer step reads

$$k = \frac{Q^{\ddagger}_{rot}}{Q^{r}_{vib}Q^{r}_{rot}} \frac{\mathrm{Corr}(\Delta)}{2\hbar\widetilde{\beta}_c \sin(\pi\beta/\widetilde{\beta}_c)} e^{-\beta\widetilde{V}_0}, \quad \text{for } \beta < \widetilde{\beta}_c, \quad (5.1)$$

where

$$Q^{r}_{vib} = \prod_{n=1}^{33} \frac{1}{2\sinh(\omega_n\beta/2)}, \quad (5.2)$$

$$\frac{Q^{\ddagger}_{rot}}{Q^{r}_{rot}} = \sqrt{\frac{I^{\ddagger}_a I^{\ddagger}_b I^{\ddagger}_c}{I^{r}_a I^{r}_b I^{r}_c}} \quad (5.3)$$

and the rest of parameters were defined in Sec. II. To obtain the rate constant of the[1,5] sigmatropic rearrangement reaction one needs to include the effects of the rapid pre-equilibrium between the unreactive s-*trans* and the reactive s-*cis* conformers and to multiply the rate constant of hydrogen transfer step by the equilibrium constant $K_{eq} = Q^{cis}/Q^{trans}$, where Q^{cis} and Q^{trans} are the partition functions of s-*cis* and s-*trans* conformers, respectively. The contribution of the latter equilibrium isotope effect (EIE) K^{H}_{eq}/K^{D}_{eq} on the overall KIE turns to be minor and constitutes 1.07 at 460 K and 1.06 at 500 K.

To determine $\widetilde{\beta}_c$, $\widetilde{V}_0$, and $E'(\widetilde{\beta}_c)$, that enter Eq. (5.1) and characterize the shape of the effective one-dimensional barrier, we search for instanton trajectories with periods $\hbar\beta$ that correspond to temperatures smaller or equal than the crossover temperature $T_c = 1/\kappa_B\beta_c$. A typical temperature dependence of instanton energies $E_{inst}(\beta)$ and abbreviated actions $W_{inst}(\beta) \equiv \oint \mathbf{P}d\mathbf{Q}$ is given in Fig. 3 for the isotopologue $D_2C(CH)_3CH_3$.

Yet, the one-dimensional potential barrier that corresponds to $\mathcal{W}_{inst}(\beta)$, $E_{inst}(\beta)$, and $W_{inst}(\beta)$, such as those in Fig. 3, is not the correct barrier along the reaction coordinate. One needs to include the effect of degrees of freedom orthogonal to the reaction coordinate.[34] As proposed in Ref. 51, one can include their effect by considering an effective one-dimensional potential barrier $\widetilde{V}(s)$ that corresponds to the Euclidian action $\widetilde{\mathcal{W}}(\beta) = \mathcal{W}_{inst}(\beta) + \hbar\beta F_{vib}(\beta)$, where $F_{vib}(\beta)$ is given by Eq. (2.4) and is the total free energy of orthogonal degrees of freedom expressed through the stability parameters λ_i. This approach was tested on several bimolecular reactions and provided rather accurate estimates of quantum reaction rate constants.[51] We follow the same procedure in this paper and calculate stability parameters λ_i along the instanton trajectories, which then provide $F_{vib}(\beta) = (1/\beta)\sum_{n=1}^{N-1} \ln(2\sinh\frac{\lambda_n(\beta)}{2})$. The behavior of

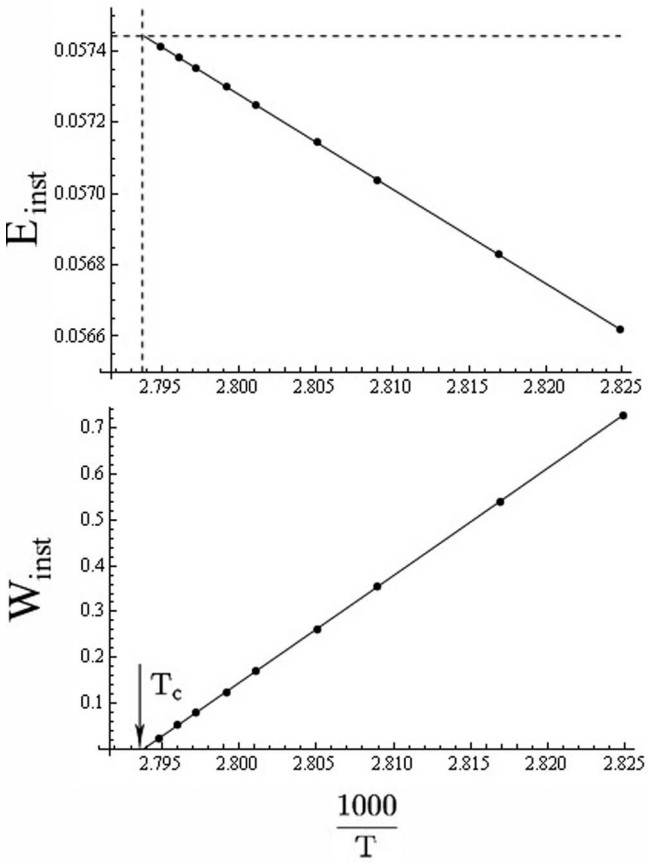

FIG. 3. The energy E_{inst} and the abbreviated action W_{inst} of $\hbar\beta$-periodic classical trajectories on the inverted PES of $D_2C(CH)_3CH_3$. The vertical dashed line and the arrow indicate the crossover temperature $T_c = 1/\kappa_B\beta_c$, defined as $W_{inst}(\beta_c) = 0$. The horizontal dashed line indicates the classical potential barrier height V_0. Temperature T is in K; E_{inst} and W_{inst} are in atomic units.

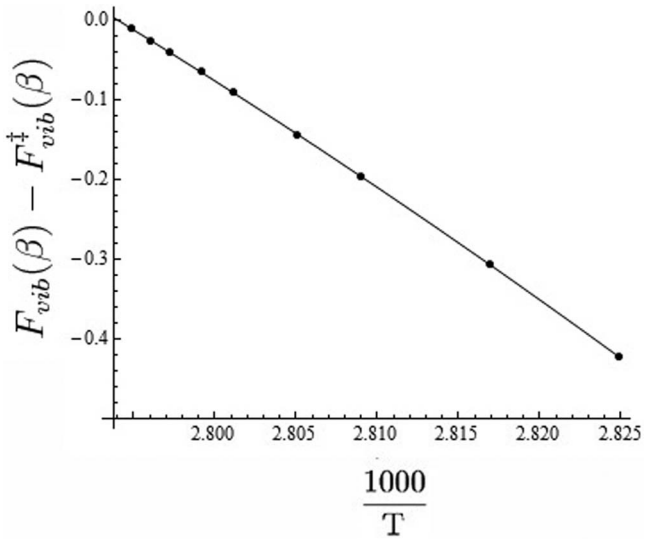

FIG. 4. The difference between $F_{vib}(\beta) = (1/\beta)\sum_{n=1}^{32} \ln(2\sinh\frac{\lambda_n(\beta)}{2})$ and its saddle point value $F^{\ddagger}_{vib}(\beta) = (1/\beta)\sum_{n=1}^{32} \ln(2\sinh\frac{\hbar\omega_j^{\ddagger}\beta}{2})$ for the isotopologue $D_2C(CH)_3CH_3$ at different temperatures $\beta = 1/\kappa_B T$. The frequencies $\omega_j^{\ddagger}$ are 32 stable vibrational frequencies at the transition state configuration. The units are kcal/mol for F_{vib} and Kelvins for T.

$F_{vib}(\beta)$ as a function of the inverse temperature β is shown in Fig. 4. It turns out that as temperature becomes lower, the value of $F_{vib}(\beta)$ becomes smaller than that at the saddle point. Physically it means that for the given EVB potential energy surface the total zero-point energy of the orthogonal degrees of freedom decreases as one moves from the saddle point to lower energies for this particular surface.

The inclusion of the orthogonal degrees of freedom changes $\mathcal{W}_{inst}(\beta)$, $E_{inst}(\beta)$, and $W_{inst}(\beta)$ to the respective $\widetilde{\mathcal{W}}(\beta) = \mathcal{W}_{inst}(\beta) + \hbar\beta F_{vib}(\beta)$, $\widetilde{E}(\beta) = E_{inst} + (d/d\beta)(\beta F(\beta))$, and $\widetilde{W}(\beta) = W_{inst}(\beta) - \hbar\beta(d/d\beta)F_{vib}(\beta)$, is shown in Figure 5 and in the Appendix. The root of $\widetilde{W}(\beta) = 0$ (as it can be seen in Fig. 5) defines the new effective crossover temperature $\widetilde{\beta}_c$ and thus the new curvature of the effective barrier along the reaction coordinate, schematically shown in Fig. 6. Since $\widetilde{\beta}_c < \beta_c$ the unstable frequency $\widetilde{\omega}_b = 2\pi/\hbar\widetilde{\beta}_c$ at the effective barrier top is higher than that $\omega_b = 2\pi/\hbar\beta_c$ of the PES. The latter can also be understood from the discussion in the previous paragraph, where we mentioned that for the used PES zero-point energy of transverse degrees of freedom turns to be maximal at the saddle point, as seen in Fig. 6.

From the extrapolation of $\widetilde{W}(\beta)$ we find the new refined crossover temperatures $\widetilde{\beta}_c = 1/\kappa_B(375\,\mathrm{K})$, for $D_2C(CH)_3CH_3$, and $\widetilde{\beta}_c = 1/\kappa_B(292\mathrm{K})$ for $H_2C(CH)_3CD_3$. Similarly we find the respective new anharmonicity parameters $\widetilde{E}'(\widetilde{\beta}_c) = -1.75 \times 10^{-3}$ a.u. and $\widetilde{E}'(\widetilde{\beta}_c) = -1.3 \times 10^{-3}$ a.u. Yet, determination of $\widetilde{V}_0$ as an extrapolation of $\widetilde{E}(\beta)$ to the point $\beta = \widetilde{\beta}_c$ is not a reliable procedure since both the rate constant and KIE exponentially depend on $\widetilde{V}_0$. Extrapolation with a second order polynomial including points in the vicinity of crossover temperature produced KIE of 8.3 at 463.25 K and 6.5 at 500 K.

To obtain more accurate estimates of KIE one should avoid the extrapolation procedure. An approximate analytical expression for $\widetilde{V}_0$ is derived in the Appendix. Assuming that the effects of asymmetry of ZPEs along the reaction coordinate s are minor, i.e., assuming that ZPE(s) = ZPE(-s), one obtains

$$\widetilde{V}_0 = V_0 + \frac{1}{\beta}\sum_{j=1}^{32} \ln\left[2\sinh\left(\hbar\omega_j^{\ddagger}\beta/2\right)\right], \qquad (5.4)$$

which coincides with the expression for the free energy at the transition state. As shown in the Appendix, for symmetric barriers, the major effect from the inclusion of orthogonal to the reaction coordinate degrees of freedom lies in reshaping of the effective 1D reaction barrier, thus resulting in the modified unstable frequency $\widetilde{\omega}_b$ at the barrier top. This new curvature of the effective barrier defines the extent of tunneling contributions to reaction rates and thus the magnitudes of KIEs. Substitution of Eq. (5.4) as well as the new curvature $\widetilde{\omega}_b = 2\pi/\hbar\widetilde{\beta}_c$ and anharmonicity $\widetilde{E}'(\widetilde{\beta}_c)$ to the semiclassical expression (2.2) results in KIEs k_H/k_D that are in good agreement with experimental as well as previous theoretical results, as seen in Table II.

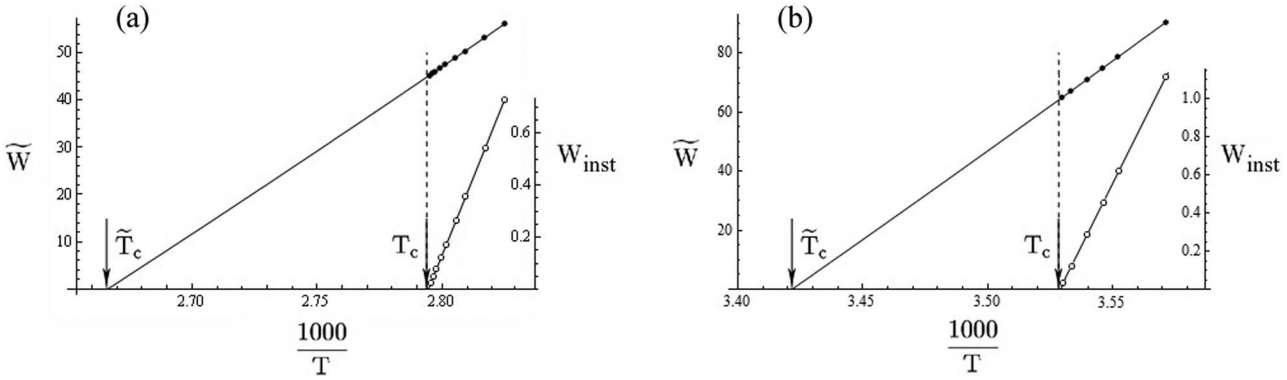

FIG. 5. The effective abbreviated action $\widetilde{W}$ (left axis, solid circles), and the instanton abbreviated action $W_{inst}(\beta)$ (right axis, open circles) as a function of the inverse temperature β for (a) $D_2C(CH)_3CH_3$ and (b) $H_2C(CH)_3CD_3$. The root of $\widetilde{W}(\beta) = 0$ defines the new crossover temperature $\widetilde{T}_c$. The original instanton crossover temperature, T_c, is shown for reference. Atomic units are used for $\widetilde{W}$ and W, and Kelvins for T.

A. Factors contributing to the calculated KIE

The analytical form of the expression (5.1) allows one to study the factors that produce the observed KIE in *cis*-1,3-pentadiene. Each term in Eq. (5.1) has a clear physical meaning and the equation can be effectively represented as a product of the following contributions. The first one is the transition state theory (TST) reaction rate constant with the barrier height $\widetilde{V}_0$ which includes zero-point energy contributions of the orthogonal to the reaction coordinate degrees of freedom:

$$k_{\mathrm{TST}} = \frac{Q^{\ddagger}_{rot}}{Q^{r}_{vib} Q^{r}_{rot}} \frac{1}{2\pi\hbar\beta} e^{-\beta \widetilde{V}_0}. \tag{5.5}$$

The second contribution is the quantum transmission coefficient for the reactive flux over the parabolic transition state barrier[81]

$$\frac{\pi\beta}{\widetilde{\beta}_c \sin\left(\frac{\pi\beta}{\widetilde{\beta}_c}\right)}, \tag{5.6}$$

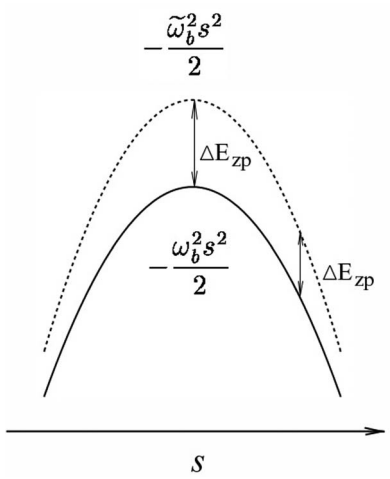

FIG. 6. Potential barrier along the reaction coordinate s. Solid line represents the effective barrier formed by one-dimensional instanton trajectories, and dashed line represents effective one-dimensional barrier $\widetilde{V}(s)$ which includes zero-point energy ΔE_{zp} contributions of the orthogonal degrees of freedom. Only the harmonic parts of the barriers are shown in figure for simplicity.

which tends to unity as β, the inverse temperature, decreases. And the third contribution,

$$\mathrm{Corr}(\Delta), \tag{5.7}$$

is the contribution of the potential barrier anharmonicity effects, i.e., the anharmonicity of the barrier along the reaction coordinate. The coefficient $\mathrm{Corr}(\Delta)$ removes the divergence of the parabolic barrier transmission coefficient in Eq. (5.6) as $\beta \to \widetilde{\beta}_c$.

Figure 7 illustrates contributions of each of the three terms in Eqs. (5.5)–(5.7) to the calculated KIE in *cis*-1,3-pentadiene. A single TST term given by Eq. (5.5) results in low KIEs as was reported previously in Ref. 53. The inclusion of the second, tunneling, term given by Eq. (5.6) already captures most of the calculated KIE, as seen in Fig. 7. The third, anharmonicity, term from Eq. (5.7), refines temperature dependence of KIE at lower temperatures.

The difference between using the effective barrier shape parameters, $\widetilde{\beta}_c$ and $\widetilde{E}'(\widetilde{\beta}_c)$, that account for the contribution of the orthogonal degrees of freedom, versus the original instanton parameters β_c and $E_{inst}(\beta_c)$ on PES is illustrated in Figure 7. This difference constitutes 20% and increases at lower temperatures. It is mostly due to the tunneling transmission coefficient of Eq. (5.6) that depends on the unstable frequency of the barrier. The latter indicates the importance of appropriate inclusion of zero-point contributions, since they influence the shape of the effective reaction barrier.

TABLE II. Experimental and theoretical kinetic isotope effects in *cis*-1,3-pentadiene for different temperatures.

T(K)	Expt.[a]	TST[b]	CVT/SCT[c]	QI[d]	SI[e]
463.25	5.3	2.51	5.2	5.4	5.8
470	5.2	2.48	4.9	5.3	5.5
478.45	5.0	2.45	4.7	5.1	5.2
500	4.7	2.36	4.1	4.3	4.6

[a]Reference 57.
[b]Reference 53.
[c]Reference 54.
[d]Reference 55.
[e]Present paper with EVB PES and $\widetilde{V}_0$ from Eq. (5.4).

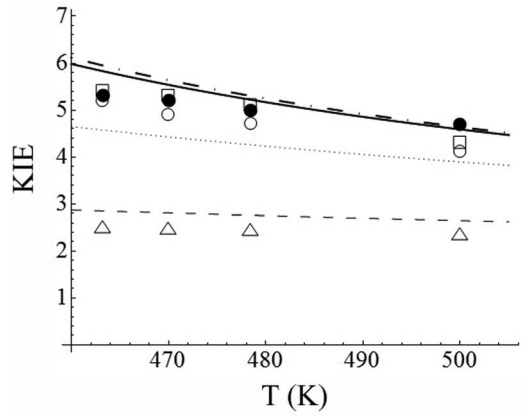

FIG. 7. H/D kinetic isotope effect as a function of temperature for the[1,5] sigmatropic rearrangement reaction of *cis*-1,3-pentadiene. Solid circles represent experimental results;[57] open triangles-transition state theory (TST) results with no tunneling;[53] open circles-CVT/SCT theory;[54] and open squares-QI theory.[55] The solid line represents semiclassical instanton results of the present paper with $\widetilde{V}_0$ from Eq. (5.4). Contributions of factors from Eqs. (5.5) to (5.7) to the semiclassical KIE: dashed line corresponds to the single TST factor (5.5); dotted-dashed line corresponds to the product of the TST (5.5) and the tunneling (5.6) factors; solid line is the product of all three factors (5.5), (5.6), and (5.7). Dotted line represents the present semiclassical results for the case when the parameters of the original PES, β_c and $E'_{inst}(\beta_c)$, are used instead of the effective parameters $\widetilde{\beta}_c$ and $\widetilde{E}'(\widetilde{\beta}_c)$.

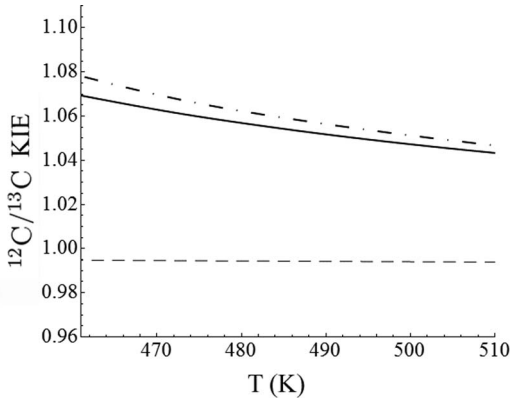

FIG. 8. $^{12}C/^{13}C$ kinetic isotope effect as a function of temperature in *cis*-1,3-pentadiene. The notation is the same as in Figure 7: solid line represents the semiclassical instanton results, dashed line represents TST results, and dotted-dashed line corresponds to the TST results with tunneling under the effective harmonic barrier.

B. Heavy atom $^{12}C/^{13}C$ KIE

We can also study the effect of isotopic replacement of carbon atoms on the rate of hydrogen transfer. Heavy atom isotope effects can be accurately measured in experiments and provide additional information on the mechanisms of chemical reactions. We calculate heavy-atom KIE as a ratio of reaction rate constants, k_{12}/k_{13}, for the reactions of H-transfer in $D_2C(CH)_3CH_3$ and in its heavier isotopologue, for this initial calculation, with all carbon atoms ^{12}C replaced by the isotopes ^{13}C. (In subsequent work using a modified method we plan to replace the C's isotopically one at a time as in the usual experiment on ^{13}C effects[82,83]) To calculate k_{13}, we search for semiclassical instantons on the same PES described in Sec. III. The optimization algorithm for instantons of k_{13} quickly converges if the instantons of k_{12}, that were found in the calculations of H/D KIEs, are taken as an initial guess. We then use the expression in Eq. (2.2) with the potential barrier height from Eq. (5.4) to calculate reaction rate constants k_{13} at different temperatures. $^{12}C/^{13}C$ KIEs were calculated in the same temperature range as that for H/D KIEs. The results of numerical calculations are shown in Figure 8.

Similarly to the discussion of Sec. V A, we can investigate the factors that constitute the calculated heavy-atom KIE. The change in zero-point vibrational energy due to the replacement of ^{12}C with ^{13}C influences the reaction barrier height, and thus the contribution of TST term, Eq. (5.5), resulting in the TST KIE of about 1.02 in the temperature range from 460 K to 500 K. However, the EIE of *trans-cis* isomerization, which constitutes 0.974 in the considered temperature range, reduces the KIE down to 0.995. The tunneling contribution, Eq. (5.6), increases KIE further to about 1.06. The inclusion of barrier anharmonicity, Eq. (5.7), refines the overall KIE, although its effect is small, as one can see in Fig. 8. We therefore conclude that quantum mechanical tunneling is the main factor that influences heavy-atom KIEs in the considered temperature range. Since the tunneling of atoms is collective and non-separable, as illustrated by instanton trajectories in Fig. 2, then it is the simultaneous hydrogen-carbon tunneling that dominantly contributes to the calculated heavy atom $^{12}C/^{13}C$ KIE. This particular collective tunneling behavior is not well-known in the enzyme field, a field where we plan to apply the present method.

VI. DISCUSSION

This paper demonstrates application of semiclassical instanton approach to calculation of KIEs in 13-atomic system. Intramolecular hydrogen transfer in *cis*-1,3-pentadiene molecule was chosen as an example. The latter can serve as a prototype of hydrogen transfer reactions in polyatomic molecules. Both experimental and theoretical studies are available for this reaction, which makes it a good test system. We showed that semiclassical instanton analysis can be efficiently applied in this 39 dimensional system, and extensions to systems of higher dimensions are straightforward.

The main idea behind the present instanton approach to the reaction rate theory[51] is a rigorous construction of the effective one-dimensional reaction barrier for any particular multidimensional PES with a first-order saddle point. This reaction barrier is constructed from the energies of tunneling trajectories, the instantons, plus effective zero-point vibrational energies of orthogonal degrees of freedom. The latter zero-point energies are rigorously accounted for in the theory via the stability parameters along the instanton trajectories. Thus constructed, the effective potential barrier has a different shape, and, in some cases, a different height than the classical reaction barrier along the minimum energy path on PES. While the absolute value of a reaction rate constant mostly depends on the height of the barrier, the ratio of rate constants, such as KIE, mostly depend on the shape of the barrier. It

is therefore a promising feature of the instanton approach to accurately reproduce KIEs, since it provides a rigorous description of the effective reaction barrier. The particular EVB PES used in the present analysis, however, did not allow one to numerically evaluate the effective barrier height $\widetilde{V}_0$. The latter is because EVB PES resulted in total zero-point vibrational energy that has maximum in the transition state configuration. Further developments of the theory are needed for this kind of systems. In the Appendix, we have derived an approximate analytical expression for $\widetilde{V}_0$ neglecting the effects of ZPE asymmetry. Since KIEs, being a ratio of two rate constants, are not very sensitive to the barrier height $\widetilde{V}_0$, the calculated H/D KIEs turn out to be in a good agreement with the experimental and the available theoretical results, as shown in Table II and Figure 7. We also studied the effect of heavy atom isotopic replacement $^{12}C \rightarrow {}^{13}C$ on the rate of hydrogen transfer in $D_2C(CH)_3CH_3$ and predicted its $^{12}C/^{13}C$ KIEs, reported in Fig. 8.

One of the main merits of the analytical form of the semiclassical expression of a reaction rate constant is that it allows one to investigate the physical mechanisms that are responsible for the observed KIEs. The analyses of both H/D and $^{12}C/^{13}C$ KIEs indicate that a significant contribution to the calculated KIEs comes from quantum mechanical tunneling of reactive flux, i.e., collective tunneling of hydrogen and carbon atoms, under the effective one-dimensional reaction barrier. Only a small portion of reactive flux tunnels in the reported temperature range of 460–500 K. Yet, it contributes a factor of about 2 to the H/D KIE. For the given EVB PES, quantum tunneling becomes the primary reaction mechanism at temperatures below 375 K for hydrogen transfer in $D_2C(CH)_3CH_3$, and at temperatures below 292 K for deuterium transfer in $H_2C(CH)_3CD_3$, as it follows from the corresponding instanton crossover temperatures.

An attractive feature of the semiclassical instanton reaction rate theory is the possibility of its integration with on the fly *ab initio* calculations of PES. The latter has been demonstrated for low-temperature systems with 21 degrees of freedom,[49] and up to 39 degrees of freedom.[47,50] Semiclassical instanton approach is therefore a promising technique for calculation of quantum mechanical reaction rate constants and kinetic isotope effects in real multiatomic systems.

ACKNOWLEDGMENTS

M.K. would like to acknowledge Dr. Jiři Vaníček for providing details of the EVB potential and Dr. Vyacheslav Bryantsev for assisting with electronic structure calculations. We are pleased to acknowledge the support of this research by the Granville Fellowship to M.K. and by grants to R.A.M. from NSF, ONR and ARO.

APPENDIX: EFFECT OF TRANSVERSE DEGREES OF FREEDOM ON REACTION BARRIER

In this Appendix the effect of orthogonal to the reaction coordinate degrees of freedom on the shape of effective potential barrier is demonstrated. For simplicity we consider the Hamiltonian of the form

$$H(s, X) = \frac{1}{2}\dot{s}^2 + V_0(s) + \sum_j \frac{1}{2}\dot{X}_j{}^2 + \frac{1}{2}\omega_j^2(s)X_j^2, \quad \text{(A1)}$$

where s is a one-dimensional coordinate along the instanton trajectory (unstable mode) and X are the orthogonal degrees of freedom (stable modes). Semiclassical instanton approach assumes that any multidimensional system with one unstable degree of freedom can be approximated with Hamiltonian of the form in Eq. (A1). The partition function that corresponds to this Hamiltonian, i.e., the barrier partition function, is

$$Z_b = \oint D[s(\tau)] \prod_{j=1}^{N-1} \oint D[X_j(\tau)] \times \exp\left(-\frac{1}{\hbar}\int_0^{\beta\hbar} d\tau \left[\frac{1}{2}\dot{s}(\tau)^2 + V_0(s(\tau)) + \sum_j \frac{1}{2}\dot{X}_j(\tau)^2 + \frac{1}{2}\omega_j^2(s)X_j(\tau)^2\right]\right). \quad \text{(A2)}$$

Integration over the harmonic coordinates X_j can be performed analytically resulting in[40]

$$\oint D[X_j(\tau)] \quad \exp\left(-\frac{1}{\hbar}\int_0^{\beta\hbar} d\tau \left[\frac{1}{2}\dot{X}_j(\tau)^2 + \frac{1}{2}\omega_j^2(s)X_j(\tau)^2\right]\right) = \frac{1}{2\sinh(\lambda_j[s(\tau)]/2)}, \quad \text{(A3)}$$

where λ_j is a stability parameter that corresponds to the solution $X_j(\tau + \beta\hbar) = X_j(\tau)\exp(\lambda_j)$ of the equation $-\partial^2 X_j/\partial\tau^2 + \omega_j^2(s(\tau))X_j = 0$.[33,40] Substituting Eq. (A3) into Eq. (A2), we get

$$Z_b = \oint D[s(\tau)] \exp\left(-\frac{1}{\hbar}\int_0^{\beta\hbar} d\tau \left[\frac{1}{2}\dot{s}(\tau)^2 + V_0(s(\tau))\right] - \frac{\sigma(s(\tau))}{\hbar}\right), \quad \text{(A4)}$$

where $\sigma(s(\tau)) = \hbar\sum_{j=1}^{N-1} \ln[2\sinh(\lambda_j(s(\tau)))]$.

We first review calculation of partition function of a one-dimensional barrier, i.e. for the case when $\sigma(s)$ is absent in Eq. (A4). For temperatures above the crossover we can use asymptotic analysis[41] and Taylor expand $V(s)$ around the barrier top $V_0 \equiv V(s_b)$ up to the quartic term

$$V(s) = V_0 - \frac{\omega_b^2}{2}(s - s_b)^2 + \frac{1}{3!}c(s - s_b)^3 + \frac{1}{4!}g(s - s_b)^4. \quad \text{(A5)}$$

Representing $\hbar\beta$-periodic quantum paths $s(\tau)$ in terms of Fourier series

$$s(\tau) - s_b = \sum_{n=-\infty}^{\infty} \widetilde{s}_n \exp(\imath\Omega_n\tau) \quad \text{(A6)}$$

with $\Omega_n = 2\pi n/\beta\hbar$, the Euclidean action S takes the following asymptotic form[41]

$$\begin{aligned}\frac{S}{\hbar} &= \int_0^{\beta\hbar} d\tau \left[\frac{1}{2}\dot{s}(\tau)^2 + V_0(s(\tau))\right] \\ &= \beta V_0 - \frac{1}{2}\beta\omega_b^2\left(\widetilde{s}_0 - \frac{c}{\omega_b^2}|\widetilde{s}_1|^2\right)^2 \\ &\quad + \beta\bar{\Omega}_2^2\left|\left(\widetilde{s}_2 + \frac{c}{2\bar{\Omega}_2^2}\widetilde{s}_1^2\right)\right|^2 \\ &\quad + \beta\bar{\Omega}_1^2|\widetilde{s}_1|^2 + \beta\frac{A}{2}|\widetilde{s}_1|^4 + \sum_{n>2}\beta\bar{\Omega}_n^2|\widetilde{s}_n|^2, \end{aligned} \tag{A7}$$

where $\bar{\Omega}_n^2 = \Omega_n^2 - \omega_b^2$ and $A = (g/2) + (c^2/\omega_b^2) - (c^2/2\bar{\Omega}_2^2)$. The result of integration over new coordinates $\widetilde{s}_j$ in the path integral $Z_b = \oint D[s]\exp(-S/\hbar)$ is the same as that for the parabolic barrier $-\omega_b^2 s^2/2$ except for the coordinate $\widetilde{s}_1$, which needs to be treated separately, and results in the additional factor Corr, $Z_b = \mathrm{Corr} Z_{pb}$,

$$\begin{aligned}\mathrm{Corr} &= \frac{\int_0^\infty d(|s_1|^2)\exp(-\beta\bar{\Omega}_1|s_1|^2 - \beta A|s_1|^4/2)}{\int_0^\infty d(|s_1|^2)\exp(-\beta\bar{\Omega}_1|s_1|^2)} \\ &= \Delta\sqrt{2\pi}\,\mathrm{erf}(-\Delta)e^{\Delta^2/2}, \end{aligned} \tag{A8}$$

where $\Delta = \bar{\Omega}_1^2\sqrt{\beta/A}$, and $Z_{pb} = (\iota/2\sin(\hbar\beta\widetilde{\omega}_b/2))\exp(-\beta V_0)$.

In a multidimensional system, the instanton approximation adds an extra term $\sigma(s(\tau))$ to the expression of the partition function in Eq. (A4). In a similar way we represent it with asymptotic series. The frequencies of orthogonal degrees of freedom, $\omega_j(s)$, can be Taylor expanded around the barrier top, i.e., the saddle point region

$$\omega_j(s) = \omega_j^\ddagger + \frac{d\omega_j}{ds}(s - s_b) + \frac{1}{2}\frac{d^2\omega_j}{ds^2}(s - s_b)^2, \tag{A9}$$

where $\omega_j^\ddagger$ is the corresponding frequency at the saddle point. Quasiclassical approximation can be then invoked[40] to express stability parameters λ_j in terms of the frequencies $\omega_j(s)$

$$\lambda_j = \int_0^{\beta\hbar} \omega_j(s(\tau))d\tau. \tag{A10}$$

Substituting here Eq. (A9) as well as Fourier representation of $s(\tau)$ from Eq. (A6) we get

$$\lambda_j = \hbar\beta\left\{\omega_j^\ddagger + \frac{d\omega_j(s_b)}{ds}\widetilde{s}_0 + \frac{1}{2}\frac{d^2\omega_j(s_b)}{ds^2}\sum_{n=-\infty}^{\infty}|\widetilde{s}_n|^2 + \cdots\right\}. \tag{A11}$$

Taylor expansion of $\ln(2\sinh(x)) \approx \ln(2\sinh(x_0)) + \coth(x_0)(x - x_0)$

$$\begin{aligned}\ln\left(2\sinh\frac{\lambda_j}{2}\right) &\approx \ln\left(2\sinh\frac{\hbar\beta\omega_j^\ddagger}{2}\right) \\ &\quad + \frac{\hbar\beta}{2}\coth\left[\frac{\hbar\beta\omega_j^\ddagger}{2}\right]\left(\frac{d\omega_j(s_b)}{ds}\widetilde{s}_0\right. \\ &\quad \left. + \frac{1}{2}\frac{d^2\omega_j(s_b)}{ds^2}\sum_{n=-\infty}^{\infty}|\widetilde{s}_n|^2 + \cdots\right) \end{aligned} \tag{A12}$$

allows one to represent σ in the form

$$\sigma = \sigma^\ddagger + \hbar\beta\left(a\widetilde{s}_0 + b\widetilde{s}_0^2 + 2b\sum_{n=1}^{\infty}|\widetilde{s}_n|^2\right), \tag{A13}$$

where

$$\sigma^\ddagger = \hbar\sum_j \ln\left(2\sinh\frac{\hbar\beta\omega_j^\ddagger}{2}\right), \tag{A14}$$

and

$$\begin{aligned} a &= \frac{\hbar}{2}\sum_j \coth\left[\frac{\hbar\beta\omega_j^\ddagger}{2}\right]\frac{d\omega_j(s_b)}{ds}, \\ b &= \frac{\hbar}{4}\sum_j \coth\left[\frac{\hbar\beta\omega_j^\ddagger}{2}\right]\frac{d^2\omega_j(s_b)}{ds^2}. \end{aligned} \tag{A15}$$

If we assume that the asymmetry of the saddle point is rather small and $d\omega_j(s_b)/ds \approx 0$ we may neglect the coefficient a in Eq. (A13). The integrand in the power of exponent in Eq. (A4) then becomes

$$\begin{aligned}&\frac{1}{\hbar}\int_0^{\beta\hbar} d\tau\left[\frac{1}{2}\dot{s}(\tau)^2 + V_0(s(\tau))\right] + \sigma(s(\tau))/\hbar \\ &= \left(\beta V_0 + \sigma^\ddagger/\hbar\right) - \frac{1}{2}\beta\widetilde{\omega}_b^2\left(\widetilde{s}_0 - \frac{c}{\widetilde{\omega}_b^2}|\widetilde{s}_1|^2\right)^2 \\ &\quad + \beta\widetilde{\Omega}_2^2\left|\left(\widetilde{s}_2 + \frac{c}{2\widetilde{\Omega}_2^2}\widetilde{s}_1^2\right)\right|^2 \\ &\quad + \beta\widetilde{\Omega}_1^2|\widetilde{s}_1|^2 + \beta\frac{\widetilde{A}}{2}|\widetilde{s}_1|^4 + \sum_{n>2}\beta\widetilde{\Omega}_n^2|\widetilde{s}_n|^2, \end{aligned} \tag{A16}$$

where $\widetilde{\Omega}_n^2 = \Omega_n^2 - \widetilde{\omega}_b^2$, $\widetilde{A} = (g/2) + (c^2/\widetilde{\omega}_b^2) - (c^2/2\widetilde{\Omega}_2^2)$, and the new effective frequency at the barrier top is $\widetilde{\omega}_b^2 = \omega_b^2 - 2b$. In cases when $b < 0$, the new curvature of the reaction barrier is larger than the original, $\widetilde{\omega}_b > \omega_b$. The latter, for instance, is the case of the EVB PES used in the present paper.

Integration over the Fourier coefficients $\widetilde{s}_j$ in Eq. (A16) can be done similarly to the one-dimensional case of Eq. (A8), resulting in the barrier partition function $Z = \widetilde{\mathrm{Corr}}\widetilde{Z}_{pb}$, where $\widetilde{Z}_{pb}$ is the partition function of an effective parabolic barrier $-\widetilde{\omega}_b^2 s^2/2$. The coefficient $\widetilde{\mathrm{Corr}}$ accounts for the anharmonicity of the barrier given by the anharmonicity constant $\widetilde{A}$. An account of higher order Taylor expansion terms in2\break Eqs. (A9) and (A12) is expected to result in Eqs. (2.2)–(2.7), while the direct evaluation of partition function path integral with asymptotic expression (A16) provides another estimate of the high-temperature barrier partition function

$$Z_b = \mathrm{Corr}(\Delta)\frac{\iota}{2\sin(\hbar\beta\widetilde{\omega}_b/2)}\exp(-\beta V_0 - \sigma^\ddagger/\hbar) \tag{A17}$$

and the corresponding reaction rate constant $kQ_r = (\widetilde{\omega}_b/2\pi)\,\mathrm{Im}Z_b$, see Ref. 41, of the form

$$kQ_r = \mathrm{Corr}(\Delta)\frac{1}{2\hbar\widetilde{\beta}_c\sin(\pi\beta/\widetilde{\beta}_c)}e^{-\beta V_0 - \sigma^\ddagger/\hbar}, \tag{A18}$$

where $\widetilde{\beta}_c = 2\pi/\hbar\widetilde{\omega}_b$.

[1] R. K. Allemann and N. S. Scrutton, *Quantum Tunnelling in Enzyme-catalysed Reactions* (Royal Society of Chemistry, Cambridge, 2009).
[2] R. A. Marcus, Philos. Trans. R. Soc. London, Ser. B **361**, 1445 (2006).
[3] Z. D. Nagel and J. P. Klinman, Chem. Rev. **106**, 3095 (2006).
[4] M. J. Sutcliffe, L. Masgrau, A. Roujeinikova, L. O. Johannissen, P. Hothi, J. Basran, K. E. Ranaghan, A. J. Mulholland, D. Leys, and N. S. Scrutton, Philos. Trans. R. Soc. B **361**, 1375 (2006).
[5] A. Kohen and J. P. Klinman, Chem. Biol. **6**, 191 (1999).
[6] J. K. Hwang and A. Warshel, J. Am. Chem. Soc. **118**, 11745 (1996).
[7] D. G. Truhlar, J. Phys. Org. Chem. **23**, 660 (2010).
[8] A. Kohen and H. H. Limbach, *Isotope Effects In Chemistry and Biology* (CRC Press, Boca Raton, FL, 2005).
[9] B. J. Bahnson and J. P. Klinman, Methods Enzymol. **249**, 373 (1995).
[10] J. Pu, J. Gao, and D. G. Truhlar, Chem. Rev. **23**, 660 (2006).
[11] F. H. Westheimer, Chem. Rev. **61**, 265 (1961).
[12] R. P. Bell, *The Tunnel Effect in Chemistry* (Chapman and Hall, 1980), p. 80.
[13] A. Wu and J. M. Mayer, J. Am. Chem. Soc. **130**, 14745 (2008).
[14] A. Wu, E. A. Mader, A. Datta, D. A. Hrovat, W. T. Borden, and J. M. Mayer, J. Am. Chem. Soc. **131**, 11985 (2009).
[15] T. F. Markle, I. J. Rhile, and J. M. Mayer, J. Am. Chem. Soc. **133**, 17341 (2011).
[16] T. F. Markle, A. L. Tenderholt, and J. M. Mayer, J. Phys. Chem. B **116**, 571 (2012).
[17] M. J. Knapp, K. Rickert, and J. P. Klinman, J. Am. Chem. Soc. **124**, 3865 (2002).
[18] M. H. V. Huynh and T. J. Meyer, Proc. Natl. Acad. Sci. U.S.A. **101**, 13138 (2004).
[19] G. M. Wieder and R. A. Marcus, J. Chem. Phys. **37**, 1835 (1962).
[20] D. G. Truhlar and B. C. Garrett, Annu. Rev. Phys. Chem. **35**, 159 (1984).
[21] G. Mills, G. K. Schenter, D. E. Makarov, and H. Jonsson, Chem. Phys. Lett. **278**, 91 (1997).
[22] W. H. Miller, Y. Z. M. Ceotto, and S. Yang, J. Chem. Phys. **119**, 1329 (2003).
[23] E. Pollak and J. L. Liao, J. Chem. Phys. **108**, 2733 (1998).
[24] G. A. Voth, D. Chandler, and W. H. Miller, J. Chem. Phys. **91**, 7749 (1989).
[25] A. Kuppermann, J. Phys. Chem. **83**, 171 (1979).
[26] R. A. Marcus, J. Chem. Phys. **45**, 4493 (1966).
[27] I. R. Craig and D. E. Manolopoulos, J. Chem. Phys. **122**, 084106 (2005).
[28] M. Ceotto and W. H. Miller, J. Chem. Phys. **120**, 6356 (2004).
[29] Application of QI approach to several bimolecular collinear reactions resulted in reaction rate coefficients which agree with the correct quantum ones to within 20%.[28]
[30] Y. Zhao, T. Yamamoto, and W. H. Miller, J. Chem. Phys. **120**, 3100 (2004).
[31] W. Wang and Y. Zhao, Phys. Chem. Chem. Phys. **13**, 19362 (2011).
[32] R. A. Marcus and M. E. Coltrin, J. Chem. Phys. **67**, 2609 (1977).
[33] W. H. Miller, J. Chem. Phys. **62**, 1899 (1975).
[34] S. Chapman, B. C. Garrett, and W. H. Miller, J. Chem. Phys. **63**, 2710 (1975).
[35] A. O. Caldeira and A. J. Leggett, Phys. Rev. Lett. **46**, 211 (1981).
[36] H. Grabert and U. Weiss, Phys. Rev. Lett. **53**, 1787 (1984).
[37] P. Hanggi and W. Hontscha, J. Chem. Phys. **88**, 4094 (1988).
[38] P. Hanggi and W. Hontscha, Ber. Bunsenges. Phys. Chem. **95**, 379 (1991).
[39] A. A. Stuchebrukhov, J. Chem. Phys. **95**, 4258 (1991).
[40] V. A. Benderskii, D. E. Makarov, and P. G. Grinevich, Chem. Phys. **170**, 275 (1993).
[41] J. Cao and G. A. Voth, J. Chem. Phys. **105**, 6856 (1996).
[42] G. V. Mil'nikov and H. Nakamura, J. Chem. Phys. **115**, 6881 (2001).
[43] S. Andersson, G. Nyman, A. Arnaldsson, U. Manthe, and H. Jonsson, J. Phys. Chem. A **113**, 4468 (2009).
[44] J. B. Rommel, T. P. M. Goumans, and J. Kastner, J. Chem. Theory Comput. **7**, 690 (2011).
[45] J. O. Richardson, S. C. Althorpe, and D. J. Wales, J. Chem. Phys. **135**, 124109 (2011).
[46] S. C. Althorpe, J. Chem. Phys. **134**, 114104 (2011).
[47] J. Meisner, J. B. Rommel, and J. Kastner, J. Comput. Chem. **32**, 3456 (2011).
[48] C. D. Schwieters and G. A. Voth, J. Chem. Phys. **108**, 1055 (1998).
[49] G. V. Mil'nikov, K. Yagi, T. Taketsugu, H. Nakamura, and K. Hirao, J. Chem. Phys. **119**, 10 (2003).
[50] T. P. M. Goumans and J. Kastner, Angew. Chem., Int. Ed. **49**, 7350 (2010).
[51] M. Kryvohuz, J. Chem. Phys. **134**, 114103 (2011).
[52] Stationary phase approximation tends to underestimate the results of exact integration. Therefore reaction rate coefficients calculated via the semiclassical instanton (SI) approach are usually smaller than the exact ones. Applications of SI approach to several bimolecular reactions[51] showed that SI rate coefficients underestimate the correct quantum rate coefficients within a factor of 2 or less. We believe that it would be possible to derive the magnitude of error of the SI by the rigorous analysis of errors of the stationary phase approximation.
[53] G. J. M. Dormans and H. M. Buck, J. Am. Chem. Soc. **108**, 3253 (1986).
[54] Y.-P. Liu, G. C. Lynch, T. N. Truong, D. Lu, D. G. Truhlar, and B. C. Garrett, J. Am. Chem. Soc. **115**, 2408 (1993).
[55] J. Vanicek and W. H. Miller, J. Chem. Phys. **127**, 114309 (2007).
[56] D. N. Peles and J. D. Thoburn, J. Org. Chem. **73**, 3135 (2008).
[57] W. R. Roth and J. Konig, Liebigs Ann. Chem. **699**, 24 (1966).
[58] M. J. Knapp and J. P. Klinman, Eur. J. Biochem. **269**, 3113 (2002).
[59] D. K. Chakravorty, A. V. Soudackov, and S. Hammes-Schiffer, Biochemistry **48**, 10608 (2009).
[60] J. Gao, K. Y. Wong, D. T. Major, A. Cembran, L. Song, Y. Lin, Y. Fan, and S. Ma, in *Quantum Tunnelling in Enzyme-Catalysed Reactions*, edited by R. Alleman and M. Scruton (RSC Publishing, Cambridge, 2009), pp. 105–131.
[61] L. D. Landau and E. M. Lifschitz, *Quantum Mechanics: Non-Relativistic Theory* (Elsevier Science, Oxford, 1991).
[62] J. S. Langer, Ann. Phys. **41**, 108 (1967).
[63] P. Pechukas in *Dynamics of Molecular Collisions, Part B*, edited by W. H. Miller (Plenum, New York, 1976).
[64] S. Coleman in *The Whys of Subnuclear Physics*, edited by A. Zichichi (Plenum, New York, 1979), p. 805.
[65] I. Affleck, Phys. Rev. Lett. **46**, 388 (1981).
[66] H. Grabert, U. Weiss, and P. Hanggi, Phys. Rev. Lett. **52**, 2193 (1984).
[67] P. S. Riseborough, P. Hanggi, and E. Freidkin, Phys. Rev. A **32**, 486 (1985).
[68] L. Chang and S. Chakravarty, Phys. Rev. B **29**, 130 (1984).
[69] G. V. Mil'nikov and H. Nakamura, Phys. Chem. Chem. Phys. **10**, 1374 (2008).
[70] The expression in curly brackets in Eq. (2.1) includes the Van-Vleck type factor that preserves normalization of real time propagators $\exp(-\imath tH/\hbar)$ and accounts for anharmonicity effects of imaginary type propagators $\exp(-\tau H/\hbar)$, i.e., the Boltzmann operator, along the trajectory, or the reaction coordinate.[41]
[71] A. Warshel and R. Weiss, J. Am. Chem. Soc. **102**, 6218 (1980).
[72] Y. T. Chang and W. H. Miller, J. Phys. Chem. **94**, 5884 (1990).
[73] J. Wang, R. M. Wolf, J. W. Caldwell, P. Kollman, and D. A. Case, J. Comput. Chem. **25**, 1157 (2004).
[74] D. A. Case, I. T. E. Cheatham, T. Darden, H. Gohlke, R. Luo, J. K. M. Merz, A. Onufriev, C. Simmerling, B. Wang, and R. Woods, J. Comput. Chem. **26**, 1668 (2005).
[75] H. B. Schlegel and J. L. Sonnenberg, J. Chem. Theory Comput. **2**, 905 (2006).
[76] JAGUAR, version 7.7, Schrodinger, LLC, New York, NY, 2010.
[77] J. K. G. Watson, Mol. Phys. **15**, 479 (1968).
[78] C. Eckart, Phys. Rev. **47**, 552 (1935).
[79] E. Hudspeth, D. A. McWhorter, and B. H. Pate, J. Chem. Phys. **109**, 4316 (1998).
[80] A. Callegari, U. Merker, P. Engels, H. K. Srivastava, K. K. Lehmann, and G. Scoles, J. Chem. Phys. **113**, 10583 (2000).
[81] R. T. Skodje and D. G. Truhlar, J. Phys. Chem. **85**, 624 (1981).
[82] L. Kupczyk-Subotkowska, J. W. H. Saunders, H. J. Shine, and W. Subotkowski, J. Am. Chem. Soc. **115**, 5957 (1993).
[83] M. P. Meyer, A. J. DelMonte, and D. A. Singleton, J. Am. Chem. Soc. **121**, 10865 (1999).